J. Phys. B: Atom. Molec. Phys., Vol. 9, No. 13, 1976. Printed in Great Britain.

Electron impact excitation of the n^1P ($n = 2$–5) and 2^3P states of helium at intermediate energies

T Scott and M R C McDowell
Department of Mathematics, Royal Holloway College, Englefield Green, Surrey, England

Received 4 March 1976, in final form 3 June 1976

Abstract. Calculations are reported on the electron impact excitation of the n^1P ($n = 2,3,4,5$) states of He from the ground state. The incident energy range covered is from threshold to 500 eV, and the calculations are carried out in the distorted-wave polarized-orbital model. Total cross sections for all $n \leqslant 5$, total differential cross sections, differential cross sections for individual magnetic sub-levels, and orientation and alignment parameters for $n = 2,3$ are presented and compared with other theoretical studies and with experiment. Excitation of He (2^3P) is briefly discussed.

1. Introduction

Much detailed experimental information is available on electron impact excitation of the n^1P states of helium: see for example de Jongh and van Eck (1971), Moustafa Moussa *et al* (1969), Donaldson *et al* (1972), Hall *et al* (1973). In particular the $1^1S \rightarrow 2^1P$ transition is an accessible, simple, allowed, electric-dipole transition often used as a standard on which absolute calibrations may be made (Chamberlain *et al* 1970). Very recently Eminyan *et al* (1973, 1974, 1975) have made electron–photon coincidence measurements in helium, following excitation of both the $n = 2$ and $n = 3$ states, which allow a determination of the relative phase (up to a sign) of the excitation amplitude of the magnetic sub-levels, $|np,M_L = \mu\rangle$, and of the differential cross sections for these sub-levels (Chutjian and Srivastava 1975, Chutjian 1976).

On the theoretical side the optical oscillator strengths are accurately known (Schiff and Pekeris 1964) as are the generalized oscillator strengths for the electric-dipole transitions (Bell *et al* 1969). Consequently the first Born approximation (FBA) total and differential cross sections can be regarded as established.

Accurate configuration-interaction many-channel calculations close to threshold have been made by Berrington *et al* (1975) but they extend only over a narrow range of energy.

Much theoretical work has been directed towards establishing good approximations at intermediate energies, that is, from a few volts above threshold to some high energy where the FBA is adequate. Important calculations at moderately high energies include a Coulomb-projected Born approximation (Hidalgo and Geltman 1972), an eikonalized distorted-wave treatment by Joachain and Vanderpoorten (1974), a second-order diagonalization procedure by Baye and Heenen (1974), an application of the second-order optical-potential model by Berrington *et al* (1973) and a multichannel eikonal approximation by Flannery and McCann (1975).

Calculations which extend to lower energies include an important distorted-wave treatment, using the Hartree–Fock potential of the target as distorting potential in both channels (Madison and Shelton 1973) and a similar treatment based on a many-body (MBT) Green's function approach (Thomas *et al* 1974, Chutjian and Thomas 1975) in which the random-phase approximation transition potential is used.

We have applied the distorted-wave polarized-orbital models (DWPO I and II) of McDowell *et al* (1973, 1974, 1975a, b) to study total cross sections for excitation of n^1P (n = 2,3,4,5), differential cross sections for n = 2 and 3 and also orientation and alignment parameters (λ,χ) for these two cases. Our calculations have been carried out for all cases in which there are experimental measurements (up to January 1976) and at some additional energies where comparison with other theoretical models is possible. Thus our results are very extensive, and may be said to form the first comprehensive theoretical treatment of 1^1S–n^1P transitions in helium, for a particular approximation other than the FBA. Only selected results can be presented here, a full account being given elsewhere (Scott 1976).

The theoretical model is briefly outlined in § 2. Results for total cross sections for n^1P (n = 2,3,4,5) are given in § 3 and compared with other calculations and experiment. Differential cross sections (n = 2,3) are discussed in § 4, alignment and orientation parameters following in § 5. This allows us to compare our results for the individual magnetic sub-level differential cross sections (n = 2,3) with recent measurements (Chutjian 1976) in § 6.

The model is applied to excitation of 2^3P in § 7, and we show that it is satisfactory above 100 eV.

Finally our conclusions are presented in § 8.

2. Theory

The basic theoretical model employed has been described in earlier papers (Scott and McDowell 1975a, b). Observable quantities are expressed in terms of the inelastic T-matrix elements

$$T_{if} = \langle \Phi_f \, V_f \, \Psi_i^+ \rangle \tag{1}$$

in the notation adopted in Scott and McDowell (1975a). Replacing the exact Ψ_i^+ by the polarized-orbital ansatz

$$\Psi_i^+ = \sum_{\substack{\text{cyclic perms} \\ 1,2,3}} [\phi_i(12) + \phi_{1s}(1)\phi_{pol}(23) + \phi_{1s}(2)\phi_{pol}(13)]F(3)S^+(12,3) \tag{2}$$

and neglecting exchange polarization terms we have

$$\begin{aligned} T_{if} &= \langle \psi_f(12,3)\, V(12,3)\, \phi_i(12)\, F(3) \rangle - \langle \psi_f(12,3)\, V(12,3)\, \phi_i(23)\, F(1) \rangle \\ &\quad + 2\langle \psi_f(12,3)\, V(12,3)\, \phi_{1s}(1)\, \phi_{pol}(23)\, F(3) \rangle \\ &= T_{if}^{D} - T_{if}^{E} + T_{if}^{DP} \end{aligned} \tag{3}$$

in terms of direct (D), exchange (E) and direct polarization (DP) matrix elements, the last of these being omitted in the simpler DWPO I model. The interaction potential may be written

$$V(12,3) = \frac{1}{r_{13}} + \frac{1}{r_{23}} - \frac{2}{r_3}. \tag{4}$$

The differential cross section for the transitions $(1s0,\ 1s0)^1S \rightarrow (1s0,\ np\mu)^1P$, $\mu = 0, \pm 1$ is

$$\frac{d\sigma_\mu(n)}{d\Omega} = \frac{1}{4\pi^2}\frac{k_f}{k_i}|T_{1s0\rightarrow np\mu}|^2 \qquad (a_0^2\,\mathrm{sr}^{-1}) \tag{5}$$

and we denote this for brevity by σ_μ. The total differential cross section is

$$\sigma = \sigma(\theta) = \sigma_0 + 2\sigma_1 \tag{6}$$

since the system has axial symmetry, and the integral cross section

$$Q_{1s0\rightarrow np\mu} = 2\int_{-1}^{+1} \sigma_\mu(\theta)\, d(\cos\theta) \qquad (\pi a_0^2). \tag{7}$$

In a coincidence experiment in which the scattered electron is detected in coincidence with the photon emitted on decay of the $2p\,^1P$ state, we can write this state after scattering as a coherent superposition of magnetic sub-levels, quantized in the collision frame with Z axis along $\hat{\boldsymbol{k}}_i$,

$$|np\rangle = b_0|1,0\rangle + b_1(|1,1\rangle - |1,-1\rangle) \tag{8}$$

in terms of angular momentum eigenstates $|LM_L\rangle$ and complex excitation amplitudes b_μ,

$$b_\mu = b_{0\mu}\,e^{i\chi_\mu} \qquad \mu = 0,1 \tag{9}$$

where the $b_{0\mu}$ are real. It is convenient to normalize these excitation amplitudes so that

$$b_{0\mu}^2 = \sigma_\mu. \tag{10}$$

Then (Macek and Jaecks 1971, Eminyan *et al* 1973) the coincidence rate per unit differential cross section is proportional to

$$N = \lambda^2 \sin^2\theta_v + (1-\lambda)\cos^2\theta_v - [\lambda(1-\lambda)]^{1/2}\cos\chi\sin 2\theta_v \tag{11}$$

in the geometry where the photon is detected at angle θ_v to the incident electron beam, in the scattering plane. Measurements of $N(\theta_v)$ give the ratio of the magnetic sub-level differential cross sections,

$$\lambda = \sigma_0/(\sigma_0 + 2\sigma_1) \tag{12}$$

and the cosine of the relative phase of these states

$$\chi = \chi_1 - \chi_0. \tag{13}$$

The matrix elements are evaluated by expanding the scattering function $F(\boldsymbol{r})$ in partial waves, and solving the adiabatic exchange equation (cf Scott and McDowell 1975a) for these; thus

$$F(\boldsymbol{r}) = k_i^{-1/2}\sum_{l=0}^{\infty} c_l \frac{U_l(k_i, r)}{r} P_l(\cos\theta_r) \tag{14}$$

where c_l is a constant independent of r and k_i and $P_l(\cos\theta)$ is an lth order Legendre function. The polarization potential is taken, consistently with our choice of the Sternheimer function for $\phi_{pol}(\boldsymbol{r}_1, \boldsymbol{r}_3)$, to be the Callaway–Temkin form (cf Duxler *et al* 1971) with effective charge Z_0 chosen to yield the correct asymptotic adiabatic dipole polarizability.

The required matrix elements may then be expressed in terms of the partial-wave contributions as

$$T_{1s0-np\mu} = \sum_{l=0}^{\infty} a_{l\mu} P_l^{|\mu|}(\cos\theta) \tag{15}$$

where θ is the scattering angle. In evaluating total cross sections it is sufficient to take

$$Q_{1s0-np\mu} = \frac{1}{\pi}\frac{k_f}{k_i}\sum_{l=0}^{l_{max}} \frac{[l(l+1)]^{|\mu|}}{2l+1} |a_{l\mu}|^2 \qquad (\pi a_0^2) \tag{16}$$

where typically l_{max} is of order 30 for convergence to 1 part in 10^4. However due to the long-range dipole character of the interaction for optically allowed s–p transitions, very many partial waves contribute to the expressions for the differential cross sections and the relative phase χ. We found that for l greater than some l_0 (again, typically, $l_0 = 30$) the partial-wave matrix elements $a_{l\mu}$ could be replaced by their Born form (DWPO I) or their polarized Born form (DWPO II), so

$$T_{1s0-np\mu} = \sum_{l=0}^{l_0} (a_{l\mu} - a_{l\mu}(\mathrm{B})) + T^{\mathrm{B}}_{1s0-np\mu} \tag{17}$$

where $T^{\mathrm{B}}_{1s0,np\mu}$ and $a_{l\mu}(\mathrm{B})$ are the Born (or polarized Born) forms of $T_{1s0,np\mu}$ and $a_{l\mu}$. In using (17) closed expressions are required for $T^{\mathrm{B}}_{1s0-np\mu}$ and $T^{\mathrm{PB}}_{1s0-np\mu}$. For calculations on He transitions to $n = 2$ and $n = 3$ we adopted the simple Hartree–Fock wavefunctions of Morse *et al* (1935) and of Goldberg and Clogston (1939) respectively. We found that using these wavefunctions, an adequate approximation could be obtained for the polarized-Born matrix element by neglecting polarization of the core throughout. The ground-state wavefunction used in all our calculations is that of Green *et al* (1954).

The resulting simplified DWPO II differential cross sections were everywhere found to be within 10% of the corresponding DWPO I result.

In calculating total cross sections for $n = 4, 5$, the dominant contributions at energies up to 400 eV arise from the first 40 partial waves and hence renders the Born correction unnecessary. For these cases we employed the fixed-core Hartree–Fock wavefunctions of Cohen and McEachran (1969) for the excited states. Full details of the analysis will be given elsewhere (Scott 1976).

3. Total excitation cross sections

We have evaluated total cross sections for the transitions

$$\mathrm{e} + \mathrm{He}(1^1\mathrm{S}) \rightarrow \mathrm{e} + \mathrm{He}(n^1\mathrm{P}) \qquad n = 2, 3, 4, 5$$

at impact energies E_i from threshold to 500 eV and compared our results with other theoretical models and with experiment. The results are shown in figures 1 to 4.

3.1. 2^1P

We have compared with six sets of experimental measurements which are in good agreement among themselves, except for the data of Moustafa Moussa *et al* (1969) and Chutjian and Srivastava (1975) which appear low. The present DWPO II results

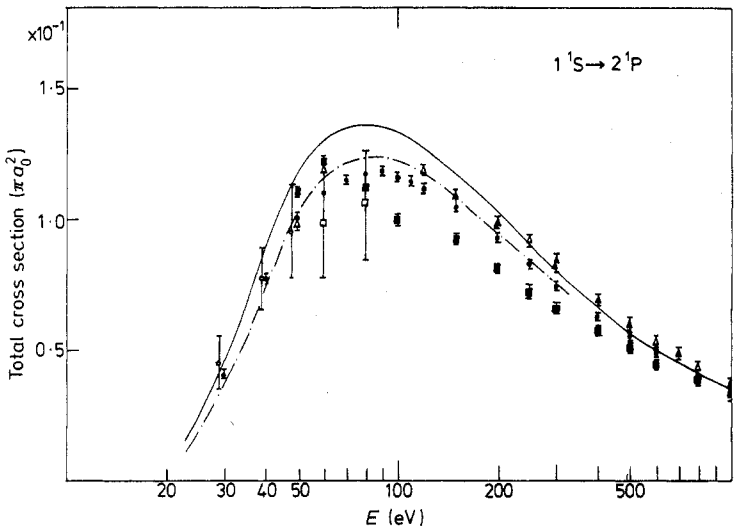

Figure 1. Total cross sections for e + He(1^1S) → e + He(2^1P), in units of πa_0^2. Theory: —— DWPO I; —·—·—·— DWPO II. Experiment: ⊟ Chutjian and Srivastava (1975); ▲ Dillon and Lassettre (1975); ⊖ Hall *et al* (1973); ● Donaldson *et al* (1972); △ de Jongh and van Eck (1971); ■ Moustafa Moussa *et al* (1969).

are in close agreement with the measurements of Donaldson *et al* (1972) at all energies considered (25 eV to 300 eV), which in turn are in good agreement with those of Hall *et al* (1973) ($E_i < 50$ eV), de Jongh and van Eck (1971) ($E_i > 80$ eV) and of Dillon and Lassettre (1975). On the other hand our DWPO I results which neglect polarization of the target in the matrix element, although retaining distorted waves, are up to 20% too high at the peak of the cross section. In table 1 we compare our theoretical results in both models with other calculated values. The table does not include the results of the Glauber approximation (Chan and Chen 1974) nor the distorted-wave treatment by Madison and Shelton (1973) both of which give total cross sections in good agreement with ours above 150 eV. At lower energies

Table 1. Theoretical total cross sections for 2^1P excitation of helium in units of $10^{-1}\,\pi a_0^2$.

E(eV)	a	b	c	d	e	f	g	h
40	0·900	0·774	0·805	1·178				1·616
50	1·166	1·027		1·304	2·15		1·942	1·694
80	1·367	1·240	1·28	1·368				1·596
100	1·333	1·220		1·312	1·55	1·99	1·455	1·484
150	1·166	1·081		1·156				1·244
200	1·015	0·947		1·021	1·05	1·26	1·004	1·069
300	0·805	0·757		0·819	0·822	0·958		0·841

[a] DWPO I.
[b] DWPO II.
[c] Many-body theory (Thomas *et al* 1974).
[d] Multichannel eikonal treatment (Flannery and McCann 1975).
[e] Second-order optical-potential (Berrington *et al* 1973).
[f] Coulomb-projected Born (Hidalgo and Geltman 1972).
[g] Second-order diagonalization (Baye and Heenen 1974).
[h] Accurate FBA (Bell *et al* 1969).

the Madison and Shelton results agree with our DWPO I values down to 70 eV and with the multichannel eikonal (Flannery and McCann 1975) at lower energies. The Glauber values appear to be in excellent agreement with the measurements of Donaldson *et al* at all energies above 50 eV.

It is convenient to summarize briefly the differences between the Madison and Shelton calculation (here after denoted by DW), the first-order many-body theory calculations of Thomas *et al* (1974), (hereafter MBT) and our own calculations. The DW and MBT models allow for distortion by the static field of the ground state in calculating both incoming and scattered waves, but DW omits exchange in this part of the calculation. Neither DW nor MBT include any polarization effects. Our treatment allows, in addition, for adiabatic dipole polarization of the incident wave (and in DWPO II of the target ground state) but omits any distortion in the final channel.

The second-order optical-potential calculation (SOP) of Berrington *et al* (1973) is an impact-parameter treatment, and its results (table 1, column e) may be unreliable below 150 eV. It has been superseded by a wave treatment, neglecting final-channel distortion, by Winters (1974) whose results at 100 eV are in close agreement with our DWPO I value.

We include the accurate FBA results of Bell *et al* (1969) in table 1 although they are in disagreement with experiment below 150 eV, overestimating badly at lower energies; clearly the CPB calculation by Hidalgo and Geltman (1972) is a less good predictor.

The multichannel eikonal results (Flannery and McCann 1975) are based on an eikonalized approximation to the ten-state close-coupling without exchange model, in an impact-parameter treatment, and again overestimate below 100 eV. We conclude that exchange effects must be included in calculating distorted waves if reasonable results are to be obtained at low energies, but that polarization and final-channel distortion are less important in determining the total cross section for this transition. Distortion of the target states is also important and is included in the MBT calculations, which can be interpreted as using random-phase approximation wavefunctions for both initial and final states, and in our DWPO II model.

3.2. 3^1P

There are fewer results available for this transition. Total cross sections have been measured by Donaldson *et al* (1972), Moustafa Moussa *et al* (1969), de Jongh and van Eck (1971) and Chutjian (1976). Their results agree well above 300 eV, but not at lower energies. In particular the data of de Jongh and van Eck show considerable structure below 200 eV, which is not seen in the other experiments nor in any of the theoretical calculations (cf figure 2). In table 2, we tabulate results in the DWPO I model.

Our DWPO I results are again some 10% higher than the DWPO II values at the peak of the cross section (80 eV), the multichannel eikonal values of Flannery and McCann (1975) falling between our two sets for $E_i > 70$ eV, but being too large at lower energies. While the DWPO I calculations are very close to the experimental values given by Donaldson *et al* (1972) the improved DWPO II results favour those of Moustafa Moussa *et al* (1969), though all agree within $\pm$ 10%. Again the second-order methods (Bransden and Issa 1975, Baye and Heenen 1974) do not appear to significantly improve on the FBA (not shown) and are in disagreement with experiment for $E_i < 150$ eV.

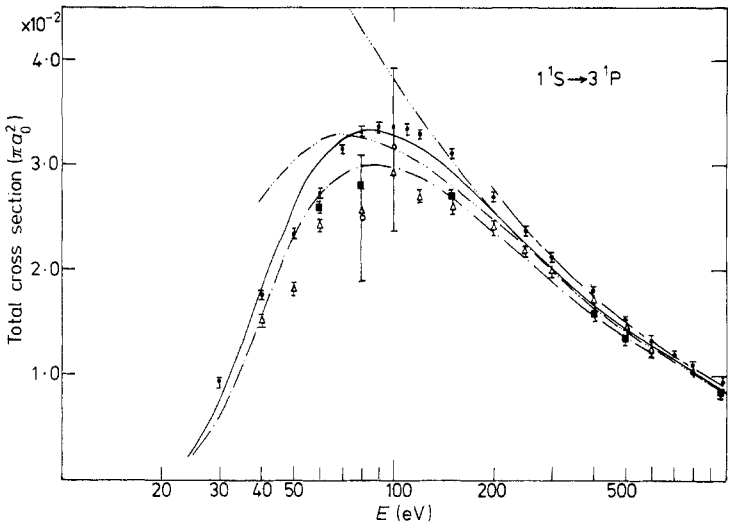

Figure 2. As figure 1, but 3^1P; experimental data of Chutjian (1976) (○) at 80 and 100 eV; other theoretical results shown are: —·—·— multichannel eikonal (Flannery and McCann 1975); —·····— Baye and Heenen (1974); ——— Bransden and Issa (1975).

Table 2. DWPO I and DWPO II total cross sections for $n^1P(n = 3,4,5)$ excitation of helium in units of $10^{-2}\ \pi a_0^2$.

E (eV)	3^1P (I)	3^1P (II)	4^1P (I)	4^1P (II)	5^1P (I)	5^1P (II)
40	1·85	1·57	0·682	0·582	0·318	0·269
50	2·64	2·30	1·02	0·882	0·486	0·420
80	3·32	2·99	1·36	1·22	0·653	0·585
100	3·29	2·99	1·35	1·22	0·649	0·588
150	2·92	2·69	1·20	1·10	0·578	0·531
200	2·55	2·37	1·04	0·965	0·502	0·465
300	2·03	1·90	0·797	0·743	0·385	0·359

3.3. 4^1P and 5^1P

Our results are compared with the multichannel eikonal calculations (Flannery and McCann 1975) and with experiment in figures 3 and 4 and tabulated in table 2. For 4^1P there are measurements by Moustafa Moussa *et al* (1969), Donaldson *et al* (1972) and de Jongh and van Eck (1971). Except for those of Moustafa Moussa *et al*, which are comparatively low, they agree closely with each other and with our DWPO results at all energies, though our DWPO I results and the measurements of de Jongh and van Eck lie 10% higher than the other data at the maximum. The multichannel eikonal results are much too high below 200 eV.

For 5^1P our calculated values were very large; this was due to the poor generalized oscillator strengths (GOS) for $1^1S \rightarrow 5^1P$ generated by the Cohen–McEachran functions. We therefore adjusted our 5^1P wavefunctions to give GOS values in agreement with the accurate results of Bell *et al* (1968), following Woollings and McDowell (1972). The calculated cross sections are shown in figure 4, where they are compared with the results of Baye and Heenen (1974) and the measurements of Moustafa Moussa *et al* (1969). Our results are uncertain above 400 eV due to the lack of convergence in partial waves, though the DWPO I results go over into the accurate

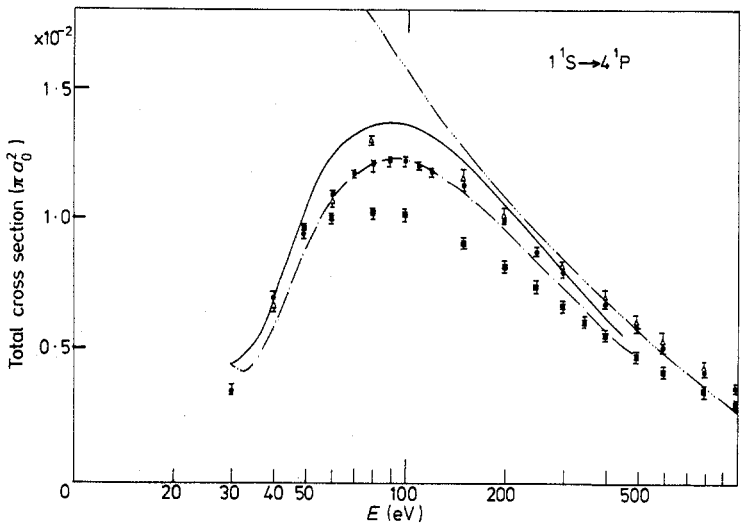

Figure 3. As figure 1, but 4^1P.

Born values at high energies. Our results at 200 eV agree well with a recent absolute measurement of Showalter and Kay (1975). This tends to confirm the suggestion of Bell *et al* (1968) that the results for this transition obtained by Moustafa Moussa *et al* should be renormalized by a factor 1·27.

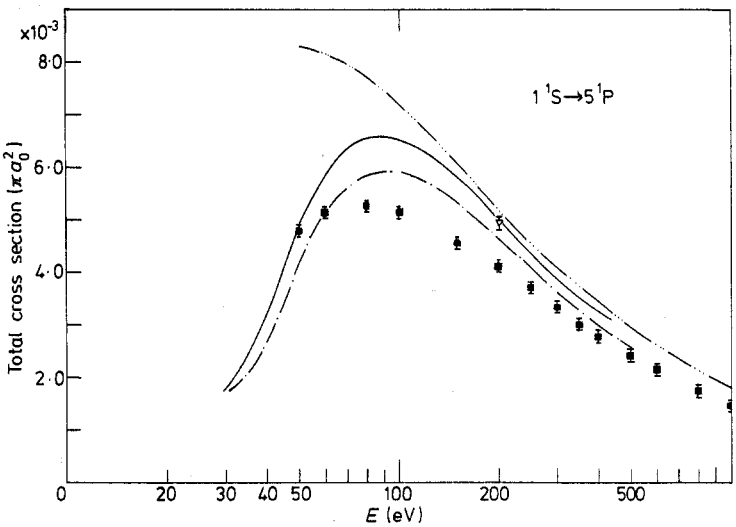

Figure 4. As figure 1, but 5^1P, (▽) experimental value of Showalter and Kay (1975).

4. Differential cross sections

There do not appear to be any experimental results for differential cross sections for 4^1P or 5^1P so we restrict our attention to the lower levels. DWPO I results only are given, except for small angles, the difference elsewhere being less than 10%. Tabulated values are presented in table 3 for 2^1P at impact energies of 40·1, 81·63, 100 and 200 eV, and in table 4 for 3^1P at impact energies of 29·2, 39·7, 100 and 200 eV.

Table 3. Differential cross sections for excitation of the helium 2^1P level at electron impact energies 40·1, 81·63, 100 and 200 eV in units of $a_0^2\,sr^{-1}$ (DWPO I).

θ (deg)	40·1 eV	81·63 eV	100 eV	200 eV
0	7·36, −1	3·93	5·43	1·36, +1
10	5·34, −1	1·28	1·24	6·62, −1
20	2·40, −1	2·20, −1	1·64, −1	3·53, −2
30	8·37, −2	3·49, −2	2·12, −2	2·47, −3
40	2·52, −2	5·71, −3	3·17, −3	4·99, −4
50	7·42, −3	1·54, −3	1·00, −3	2·64, −4
60	2·85, −3	9·26, −4	6·55, −4	1·70, −4
70	1·78, −3	7·22, −4	4·97, −4	1·13, −4
80	1·41, −3	5·73, −4	3·83, −4	8·02, −5
90	1·11, −3	4·49, −4	2·95, −4	5·77, −5
100	8·26, −4	3·53, −4	2·32, −4	4·50, −5
110	5·89, −4	2·82, −4	1·87, −4	3·50, −5
120	4·17, −4	2·27, −4	1·53, −4	2·91, −5
130	3·10, −4	1·89, −4	1·29, −4	2·42, −5
140	2·55, −4	1·64, −4	1·10, −4	2·15, −5
150	2·36, −4	1·43, −4	9·77, −5	1·91, −5
160	2·37, −4	1·26, −4	8·89, −5	1·77, −5
170	2·42, −4	1·23, −4	8·42, −5	1·72, −5
180	2·45, −4	1·28, −4	8·43, −5	1·59, −5

‚*n* denotes the power of ten by which entry is to be multiplied.

4.1. 2^1P

At the lowest energies for which we have data, $E_i = 29{\cdot}6$ eV and $E_i = 40{\cdot}1$ eV, our calculated values agree closely with the MBT results at angles between 30° and 60°. We obtain a cross section much too low at large angles, where MBT (Thomas *et*

Table 4. Differential cross sections for excitation of the helium 3^1P level at electron impact energies 29·2, 39·7, 100 and 200 eV in units of $a_0^2\,sr^{-1}$ (DWPO I).

θ (deg)	29·2 eV	39·7 eV	100 eV	200 eV
0	2·20, −2	1·24, −1	1·12	2·87
10	1·96, −2	9·60, −2	3·08, −1	1·82, −1
20	1·41, −2	4·91, −2	4·73, −2	1·14, −2
30	8·45, −3	1·94, −2	6·74, −3	8·21, −4
40	4·39, −3	6·47, −3	1·01, −3	1·47, −4
50	2·06, −3	2·01, −3	2·85, −4	7·42, −5
60	9·20, −4	7·55, −4	1·79, −4	4·80, −5
70	4·26, −4	4·49, −4	1·39, −4	3·21, −5
80	2·21, −4	3·53, −4	1·08, −4	2·27, −5
90	1·30, −4	2·78, −4	8·40, −5	1·64, −5
100	8·30, −5	2·04, −4	6·58, −5	1·27, −5
110	5·93, −5	1·40, −4	5·28, −5	9·89, −6
120	5·38, −5	9·33, −5	4·30, −5	8·21, −6
130	6·39, −5	6·60, −5	3·59, −5	6·84, −6
140	8·50, −5	5·37, −5	3·05, −5	6·07, −6
150	1·11, −4	5·10, −5	2·69, −5	5·39, −6
160	1·35, −4	5·28, −5	2·43, −5	4·98, −6
170	1·52, −4	5·55, −5	2·30, −5	4·84, −6
180	1·59, −4	5·67, −5	2·24, −5	4·50, −6

‚*n* denotes the power of ten by which entry is to be multiplied.

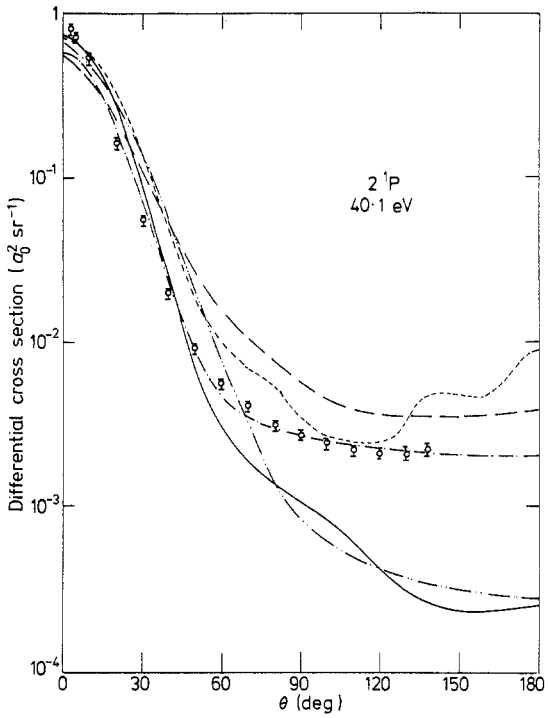

Figure 5. Differential cross section for excitation of 2^1P at 40·1 eV, in units of $a_0^2\,sr^{-1}$. The experimental data shown are those of Truhlar *et al* (1973). Theory: ——— DWPO I; —·—·— MBT (Thomas *et al* 1974); —··—··— multichannel eikonal (Flannery and McCann 1975); ------ close-coupling (Truhlar *et al* 1973); ———— distorted-wave (Madison and Shelton 1973).

al 1974) is very successful—this is probably attributable to our neglect of distortion in the final channel. Exchange–polarization effects, neglected in both calculations, must therefore be relatively unimportant in these cases. Our results are compared with the absolute experimental data of Truhlar *et al* (1973), which are in close agreement with those of other experimental groups (e.g. Hall *et al* 1973) in figure 5, for $E_i = 40{\cdot}1$ eV. Our values and those of Flannery and McCann (1975) are clearly inadequate for $\theta > 60°$. The close-coupling calculations of Truhlar *et al* (1973) show characteristic oscillations indicating a lack of convergence in the partial-wave sums, and the distorted-wave treatment of Madison and Shelton (1973) compares less well with experiment than the MBT version. However our small-angle cross sections are more accurate than those obtained in other models (figure 6) at both these energies, where they are in close accord with both sets of absolute measurements ($\theta < 30°$). At higher energies (80 eV, 100 eV) they again agree well with experiment (80 eV, Chutjian and Srivastava 1975; 100 eV Chamberlain *et al* 1970, Suzuki and Takayanagi 1973) the DWPO II results at 100 eV being below (and in better agreement with experiment) than DWPO I, which in turn is superior to the accurate FBA values (Bell *et al* 1969) (figure 7).

The same general pattern is seen at higher energies: DWPO calculations giving accurate 2^1P differential cross sections at small angles, $\theta < \theta_0$ and θ_0 decreasing with increasing impact energy, being only 30° at 200 eV. Similar behaviour was noted in the models considered by Truhlar *et al* (1970). The results we obtain are a factor

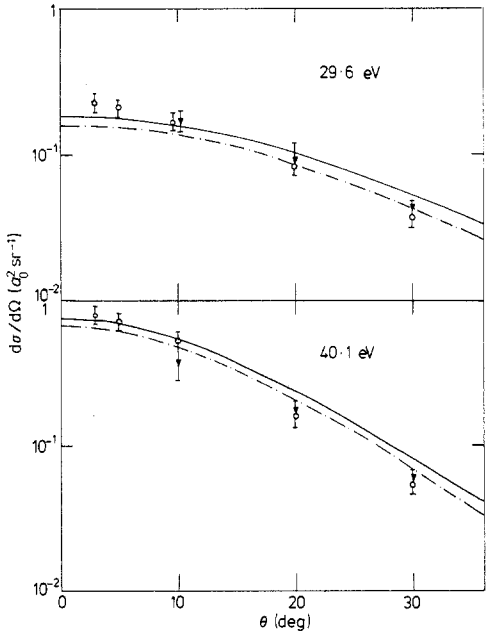

Figure 6. Small-angle differential cross section for 2^1P at 29·6 and 40·1 eV, in a_0^2 sr^{-1}. The solid curves are our DWPO I and chain curves DWPO II results. The experimental data are those of Truhlar *et al* (1973) (○) and Hall *et al* (1973) (▲).

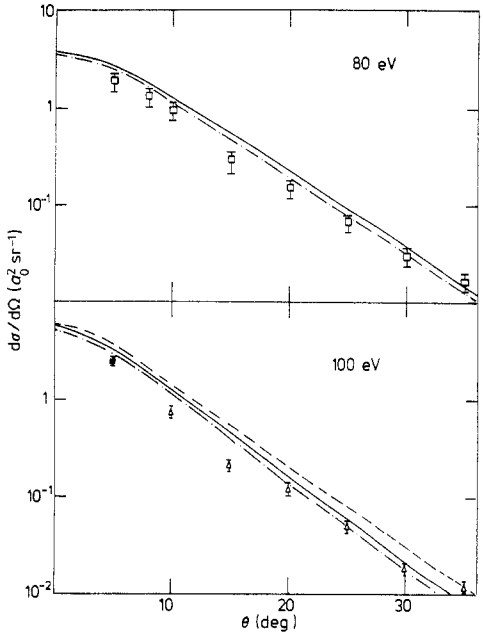

Figure 7. As figure 6, but at 80 and 100 eV. The broken curve is the first Born approximation (Bell *et al* 1969). The experimental data at 100 eV is due to Chamberlain *et al* (1970) (■) at 5° and Suzuki and Takayanagi (△) (1973), and at 80 eV due to Chutjian and Srivastava (1975) (□).

of two below the experimental values of Suzuki and Takayanagi (1973) or Opal and Beaty (1972) at 150° and 200 eV, whereas the distorted-wave model of Madison and Shelton (1973), which treats initial and final channels on an equivalent footing, is in excellent agreement with experiment at this energy and angle.

4.2. 3^1P

The pattern here is very similar though there are fewer experimental results. Our calculated small-angle cross sections at 29·2 and 39·7 eV are compared with the measurements of Chutjian and Thomas (1975) in figure 8, there being essentially complete agreement, except at 5° and 29·2 eV where our result is low compared with experiment.

Our good total cross section values are undoubtedly attributable to our achieving accurate small-angle differential cross sections, and this in turn is due to our accurate treatment of the long-range adiabatic polarization interaction. The comparison with other distorted-wave treatments (Madison and Shelton 1973, MBT) which do not include polarization, but do treat initial and final channels on an equal basis and include exchange, and with the multichannel eikonal treatment of Flannery and McCann who, neglecting exchange, treat both channels on an equivalent footing and take much of the polarization interaction into account, is instructive. The correct treatment of polarization is apparently essential in small-angle s–p scattering, while for large-angle scattering, successful prediction requires allowance for distortion in both channels, and an adequate treatment of exchange. An interesting comparison

can be made with the two-state ($1^1S, 2^1P$) close-coupling calculation of Truhlar *et al* (1973). Their calculated 2^1P differential cross sections at 29 eV are substantially larger than our values or the experimental results. At 39 eV their results are in close agreement with ours for $\theta \leqslant 10°$, but again lie much higher than our values or experiment at larger angles and appear unreliable due to lack of partial-wave convergence for $\theta > 60°$.

The close-coupling calculation is the only one which includes exchange-polarization effects (though not completely), and the above comparison suggests that these may not be significant at very small angles.

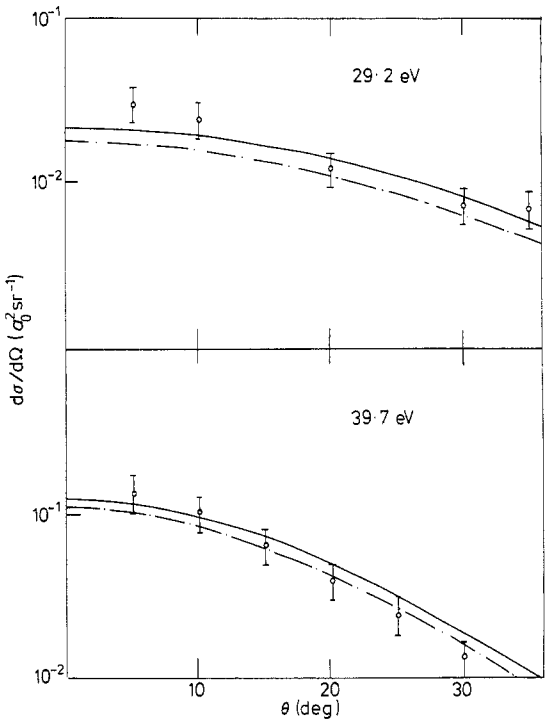

Figure 8. As figure 6, but 3^1P at 29·2 and 39·7 eV. Experimental data of Truhlar *et al* (1973).

5. Orientation and alignment effects

We have calculated λ, the ratio of the magnetic sub-level differential cross sections, and $|\chi|$, where χ is the relative phase defined in §2, for 2^1P at 40, 60, 80, 100 and 200 eV, and $0 \leqslant \theta \leqslant 180°$, and for 3^1P at 50, 80, 100 and 200 eV for the same range of angles. Our results are given in tables 5 and 6. We compare them with the experimental values of Eminyan *et al* (1974, 1975) and other theoretical models in figures 9–12. Figure 9 shows $\lambda(2^1P)$ at 40 and 60 eV, the full curve being our DWPO I result, the other calculations shown being the many-body theory result (Taylor and Thomas 1974†), the distorted-wave calculation of Madison and Shelton (1973), and the ten-channel eikonal treatment of Flannery and McCann (1975). The

† Private communication to Eminyan *et al* (1974) from H S Taylor.

Table 5. Orientation and alignment parameters for excitation of the helium 2^1P state at electron impact energies 40, 80, 100 and 200 eV (DWPO I).

	λ				$\lvert\chi\rvert$ (rad)			
θ (deg)	40 eV	80 eV	100 eV	200 eV	40 eV	80 eV	100 eV	200 eV
0	1·000	1·000	1·000	1·000				
5	0·958	0·790	0·693	0·345	8·78, −2	4·85, −2	4·33, −2	4·09, −2
10	0·855	0·518	0·406	0·175	1·03, −1	8·44, −2	8·82, −2	1·19, −1
20	0·614	0·301	0·252	0·206	1·71, −1	2·41, −1	2·76, −1	3·92, −1
30	0·430	0·279	0·297	0·557	3·15, −1	5·71, −1	6·56, −1	8·49, −1
40	0·292	0·384	0·524	0·927	6·18, −1	1·20	1·35	2·26
50	0·198	0·589	0·714	0·731	1·29	2·23	2·52	3·36
60	0·254	0·595	0·599	0·506	2·35	3·21	3·38	3·58
70	0·428	0·492	0·445	0·308	3·12	3·70	3·73	3·68
80	0·513	0·387	0·315	0·172	3·57	3·95	3·94	3·84
90	0·502	0·294	0·217	0·076	3·82	4·15	4·17	4·21
100	0·432	0·221	0·154	0·053	3·97	1·89	1·78	1·39
110	0·323	0·185	0·143	0·096	2·16	1·54	1·35	7·76, −1
120	0·210	0·202	0·194	0·204	1·85	1·16	9·53, −1	4·81, −1
130	0·171	0·289	0·303	0·350	1·25	8·48, −1	6·89, −1	3·54, −1
140	0·290	0·441	0·462	0·541	6·83, −1	6·37, −1	5·33, −1	2·79, −1
150	0·530	0·616	0·653	0·696	4·05, −1	5·12, −1	4·41, −1	2·40, −1
160	0·774	0·805	0·825	0·873	2·79, −1	4·45, −1	3·84, −1	2·28, −1
170	0·941	0·954	0·956	0·958	2·21, −1	4·22, −1	3·71, −1	1·91, −1
180	1·000	1·000	1·000	1·000				

,*n* denotes the power of ten by which entry is to be multiplied.

Table 6. Orientation and alignment parameters for excitation of the helium 3^1P state at electron impact energies 50, 80, 100 and 200 eV (DWPO I).

	λ				$\lvert\chi\rvert$ (rad)			
θ (deg)	50 eV	80 eV	100 eV	200 eV	50 eV	80 eV	100 eV	200 eV
0	1·000	1·000	1·000	1·000				
5	0·939	0·822	0·733	0·385	7·71, −2	5·22, −2	4·59, −2	4·10, −2
10	0·800	0·564	0·448	0·195	9·57, −2	8·50, −2	8·69, −2	1·14, −1
20	0·532	0·328	0·271	0·205	1·78, −1	2·26, −1	2·58, −1	3·66, −1
30	0·368	0·283	0·291	0·508	3·56, −1	5·24, −1	6·06, −1	8·02, −1
40	0·263	0·349	0·474	0·919	7·44, −1	1·12	1·26	2·03
50	0·229	0·542	0·694	0·751	1·58	2·13	2·40	3·34
60	0·376	0·599	0·612	0·521	2·66	3·18	3·36	3·59
70	0·532	0·520	0·468	0·322	3·41	3·74	3·77	3·71
80	0·563	0·430	0·348	0·183	3·82	4·01	4·00	3·87
90	0·528	0·347	0·254	0·085	4·04	4·20	4·22	4·22
100	0·458	0·278	0·193	0·059	2·10	1·87	1·77	1·42
110	0·370	0·239	0·178	0·099	1·94	1·58	1·40	8·15, −1
120	0·296	0·248	0·220	0·204	1·67	1·26	1·04	5·07, −1
130	0·284	0·320	0·319	0·350	1·29	9·64, −1	7·79, −1	3·72, −1
140	0·381	0·457	0·473	0·539	8·98, −1	7·46, −1	6·11, −1	2·93, −1
150	0·573	0·624	0·653	0·696	6·42, −1	6·09, −1	5·07, −1	2·52, −1
160	0·784	0·807	0·829	0·871	5·02, −1	5·31, −1	4·49, −1	2·36, −1
170	0·941	0·953	0·954	0·959	4·32, −1	4·98, −1	4·14, −1	2·02, −1
180	1·000	1·000	1·000	1·000				

,*n* denotes the power of ten by which entry is to be multiplied.

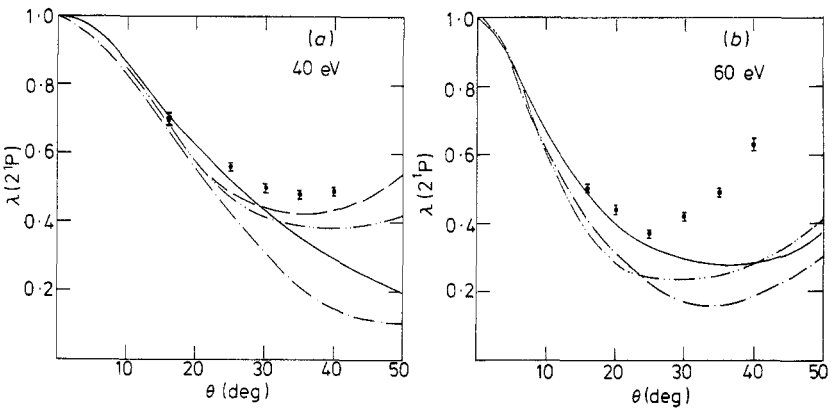

Figure 9. Ratio $\lambda = \sigma_0/(\sigma_0 + 2\sigma_1)$ of magnetic sub-level differential cross sections for 2^1P at (*a*) 40 and (*b*) 60 eV. Theory: ——— DWPO I; —·—·—·— MBT (Taylor and Thomas 1974); —··—··— multichannel eikonal (Flannery and McCann 1975); — — — distorted-wave (Madison and Shelton 1973). Experiment: ● Eminyan *et al* (1974).

experimental data are available only for a small range of angles, but it appears that all the theories are in good agreement with them and with each other for $\theta < 15°$. At 40 eV the distorted-wave results remain good out to 50°, the other models underestimating, though the multichannel eikonal is superior to ours and to the many-body theory results. At 60 eV the picture changes, our results being in the best agreement with experiment, but that agreement extending only to $\theta < 25°$, while no distorted-wave result is available. The results for 80 and 100 eV again support Madison and Shelton's treatment, our calculations being close to theirs for $\theta < 20°$, but underestimating at larger angles. At 200 eV (not shown) we are in agreement with experiment (which is available at only two angles, 16° and 20°) and with Madison and Shelton out to 40° and the multichannel eikonal results which agree with the eikonal DWBA theory (but being much too low) at angles below 25°, improving in accuracy at larger angles.

The results for $|\chi(2^1P)|$ show a somewhat different picture, as may be seen from figure 10 (80 and 100 eV). The trend of the experimental data is best represented

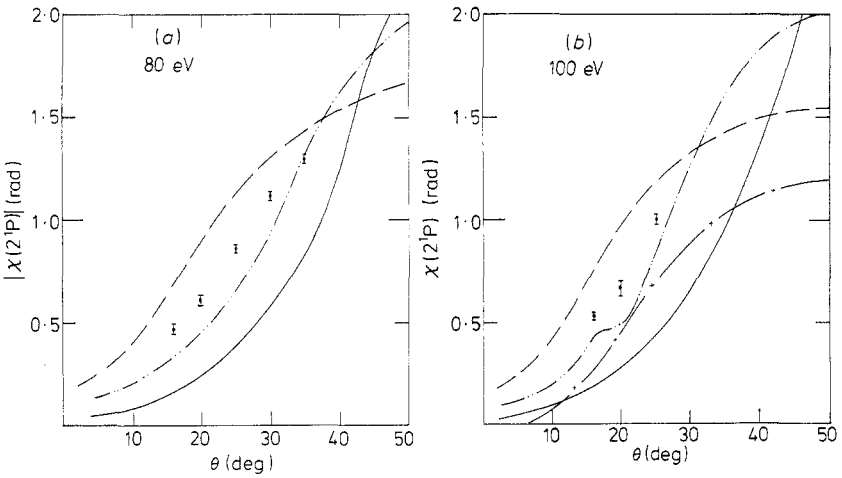

Figure 10. As figure 9, but the modulus of the relative phase, $|\chi(2^1P)|$ at (*a*) 80 and (*b*) 100 eV. —+— eikonal DWBA (Joachain and Vanderpoorten 1974).

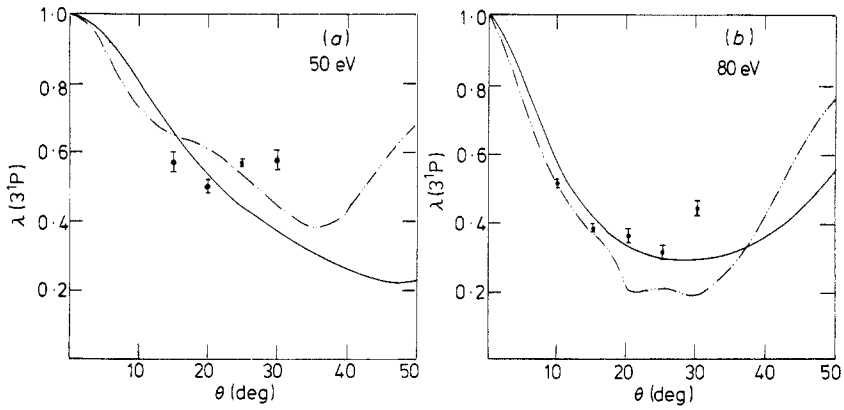

Figure 11. As figure 9, but $\lambda(3^1P)$ at (*a*) 50 and (*b*) 80 eV. The experimental data (●) are those of Eminyan *et al* (1975).

by the multichannel eikonal treatment, our results being too low, and the unpolarized distorted-wave calculations too high. These latter show a marked similarity in shape to the results of an eikonal distorted-wave calculation by Joachain and Vanderpoorten (1974), though that calculation substantially underestimates. Comparison at other energies (Scott 1976) confirms this assessment, except that at 200 eV the eikonal distorted-wave results are in as good agreement or better with experiment at 16° and 20° as are Flannery and McCann's data. The multichannel eikonal results show structure at 100 eV near 20° not resolved by experiment, nor seen in other calculations.

Some results for 3^1P are shown in figures 11 and 12. First in figure 11 we compare our results for $\lambda(3^1P)$ with experiment (Eminyan *et al* 1975) and with the multichannel eikonal treatment, at 50 and 80 eV. There appears to be some scatter in the experimental results at 50 eV, making it difficult to compare them with theory. At 80 eV both calculations are in accord with experiment at $\theta < 15°$, ours remaining good out to 25°, but giving a much lower value than experiment at 30°. Again the multichannel eikonal calculation shows considerable structure, whereas our prediction is

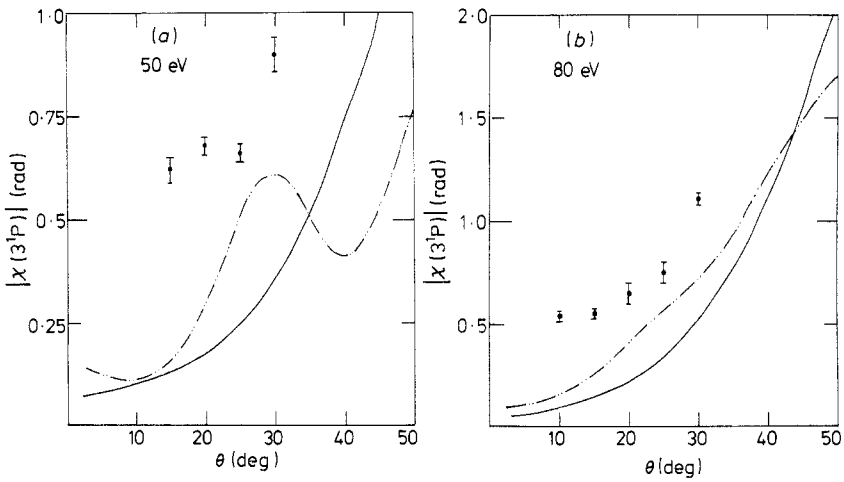

Figure 12. As figure 9, but $|\chi(3^1P)|$ at (*a*) 50 and (*b*) 80 eV, with data (●) of Eminyan *et al* (1975).

smooth. At 100 eV (not shown, but see Scott 1976) the relation of the two models is similar, DWPO being closer to experiment, but underestimating for $\theta > 20°$. Again the relative success of the two theories is reversed when we compare them with measurements of $|\chi(3^1P)|$, figure 12, though neither is very successful at 50 eV, and both underestimate at 80 eV; Flannery and McCann's results are close to the experimental values at 100 eV (not shown).

Clearly measurements of λ and χ provide a very sensitive test of theoretical models, and the work of Eminyan *et al* goes a long way to persuading us that no satisfactory theory for these processes ($1^1S \rightarrow 2^1P, 3^1P$) at intermediate energies yet exists, though an independent experimental confirmation is desirable.

6. Differential cross sections for magnetic sub-levels

Electron–photon coincidence measurements such as those of Eminyan *et al* give λ and $|\chi|$, and together with a measurement of $\sigma = \sigma_0 + 2\sigma_1$ can be combined to yield values for σ_0 and σ_1 separately (Chutjian and Srivastava 1975, Chutjian 1976).

Thus for excitation to n^1P,

$$\sigma_0 = \lambda\sigma$$

and

$$\sigma_1 = \tfrac{1}{2}(1 - \lambda)\sigma,$$

all quantities being functions of angle and incident energy. Detailed comparison with several theoretical models has been made by Chutjian and Srivastava for 2^1P at 60 and 80 eV, and by Chutjian for 3^1P at 80 and 100 eV. Our results for 3^1P at 100 eV are compared with experiment and the multichannel eikonal results in figure 13, at scattering angles $\theta < 30°$. Our agreement with experiment is essentially perfect out to 26°, whereas the ten-channel eikonal treatment which is equally successful

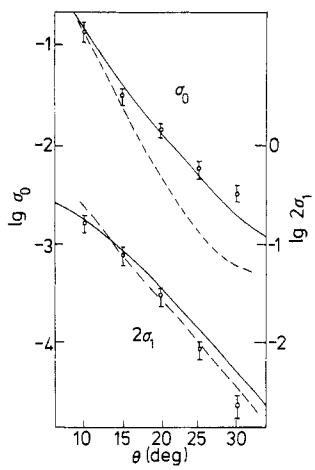

Figure 13. Individual magnetic sub-level cross sections σ_0 and $2\sigma_1$, in units of $a_0^2\,sr^{-1}$, for 3^1P at 100 eV, after Chutjian (1976), by permission. The full curves are the DWPO I results of this paper, the broken curves the multichannel eikonal (Flannery and McCann 1975).

for σ_1, fails badly for σ_0 at $\theta > 14°$. The pattern in other cases is similar. The disagreement between DWPO I and multichannel eikonal results has already been noted for H(3p) (Syms *et al* 1975).

7. Differential cross sections for excitation of 2^3P

We have also applied our model to calculate total and differential cross sections for

$$e + He(1^1S) \rightarrow e + He(2^3P).$$

Our results at low energies (below 80 eV) are in poor agreement with experiment, and are reported elsewhere (Scott 1976). Tabular values of the differential cross section at 81·63 and 200 eV are given in table 7. Our total cross section is somewhat lower than that obtained by Thomas *et al* (1974) and reproduces the trend of the experimental data, including the maximum at 35 eV, but is a factor of two too large at low energies (Scott 1976). Our results at 81·63 eV, are compared in figure 14 with the many-body theory calculations of Thomas *et al* (1974) and the measurements of Chutjian and Srivastava (1975) and of Opal and Beaty (1972). We agree well with the many-body theory results at angles out to 90°, but both theories overestimate at angles less than 40°, though our results are in reasonable agreement with Opal and Beaty's data out to 110°.

At energies below 80 eV neither the DWPO nor the MBT model is successful. At 100 eV we find agreement in general behaviour with the measurements of Suzuki and Takayanagi (1973), though these show considerable structure at intermediate angles not present in our results.

Table 7. Differential cross sections for excitation of the helium 2^3P level at electron impact energies 81·63 and 200 eV in units of a_0^2 sr^{-1} (DWPO I).

θ (deg)	81·63 eV	200 eV
0	1·70,−2	1·48,−3
10	1·68,−2	1·78,−3
20	1·47,−2	1·20,−3
30	1·03,−2	4·89,−4
40	6·06,−3	1·74,−4
50	3·23,−3	6·31,−5
60	1·64,−3	2·42,−5
70	8·25,−4	1·00,−5
80	4·21,−4	4·57,−6
90	2·27,−4	2·39,−6
100	1·38 −4	1·47,−6
110	9·68,−5	1·07,−6
120	7·80,−5	8·68,−7
130	6·87,−5	7·56,−7
140	6·31,−5	6·84,−7
150	5·90,−5	6·33,−7
160	5·59,−5	5·97,−7
170	5·39,−5	5·76,−7
180	5·32,−5	5·69,−7

,*n* denotes the power of ten by which entry is to be multiplied.

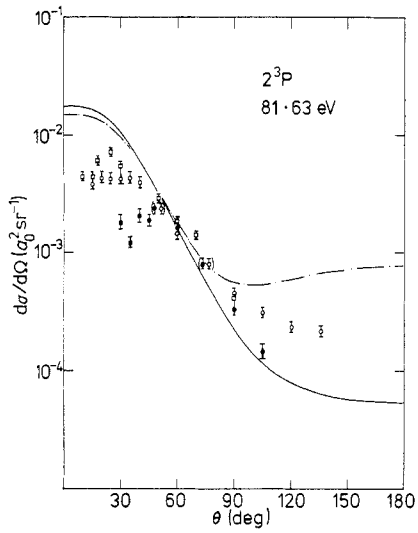

Figure 14. Differential cross section for 2^3P at 81·63 eV. The full curve is the DWPO I result, the chain curve the MBT result (Thomas *et al* 1974). The experimental points are those of Opal and Beaty (1972) (●), Chutjian and Srivastava (1975) (○) and Yagishita *et al* (1976) (□).

By 200 eV we obtain very good agreement with the available experiments (Yagishita *et al* 1976) which however are restricted to $\theta \leqslant 40°$, (cf figure 15). Our results at angles greater than 60° show appreciable sensitivity to the details of the 2^3P wavefunction adopted, values being given both for the Cohen–McEachran fixed-core Hartree–Fock function and a simpler representation of the Hartree–Fock solution due to Morse *et al* (1935).

The poor performance at energies below 100 eV of current theoretical models can be attributed to the fact that the direct matrix elements (which include second-

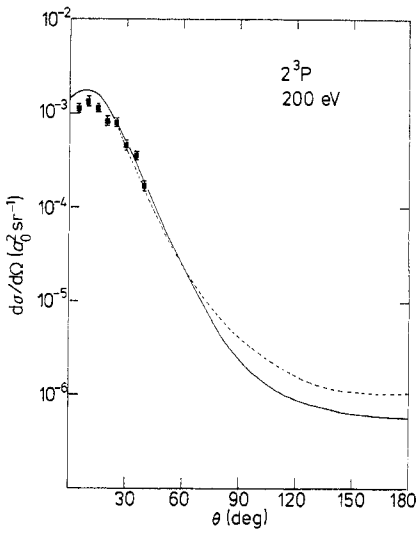

Figure 15. As figure 14, but at 200 eV. The full curve is DWPO I with a Cohen–McEachran wavefunction and the broken curve is DWPO I with a Morse Hartree–Fock 2^3P wavefunction. The experimental data (■) are those of Yagishita *et al* (1976).

order effects) vanish for singlet–triplet transitions, while no second-order effects are included in the dominant exchange matrix element.

8. Conclusions

We have calculated total excitation cross sections for the transitions $1^1S \rightarrow n^1P$ ($n = 2,3,4,5$) in helium at energies from threshold to 500 eV in a distorted-wave polarized-orbital model, and presented a detailed investigation of total differential cross sections, orientation and alignment parameters, and differential cross sections for individual magnetic sub-levels for $n = 2,3$.

Comparison of our results with differential cross section measurements suggests that our model is very accurate for scattering angles $\theta < 30°$. This suggests that our total cross sections are also accurate from just above threshold to the Born region, and this is confirmed by direct comparison with experiment.

Our model, which includes exchange and polarization effects, but not final-channel distortions, gives relatively poor agreement with measured differential cross sections for $\theta > 30°$. Surprisingly, in this angular range it agrees best with the results of a ten-state multichannel eikonal calculation by Flannery and McCann (1975), who do not include exchange. Comparison with the distorted-wave calculations of Madison and Shelton (1973) (who include exchange in the matrix element, but calculate their distorted waves in the static field of the target and also allow for final-channel distortion) and with the similar many-body theory calculations of Thomas *et al* (1974) (which differ primarily in calculating their distorted waves with exchange in the Hartree–Fock field of the target) suggests that allowance for final-channel distortion is more important than polarization effects in predicting large-angle differential cross sections.

Comparison of our results, and those of other models, with the measured orientation and alignment parameters λ and $|\chi|$ allows no clear conclusion other than that there is no available theoretical model which gives a consistent agreement with experiment. Work on improving our model by consistently including exchange–polarization effects both in calculating the distorted waves and in the matrix elements is well advanced.

Our close agreement with the recent measurements of the 2^3P differential cross section at 200 eV ($\theta \leqslant 40°$) suggests that exchange–polarization and other non-adiabatic effects are unimportant at this energy, except perhaps at large scattering angles. Extension of the measurements to such angles would be helpful.

Acknowledgments

We are indebted to Dr A Chutjian for permission to adopt figure 13 from his preprint. One of us (TS) was the holder of an SRC Research Training Grant during the course of this work.

References

Baye D and Heenen P-H 1974 *J. Phys. B: Atom. Molec. Phys.* **7** 938–49
Bell K L, Kennedy D J and Kingston A E 1968 *J. Phys. B: Atom. Molec. Phys.* **1** 204–17

——1969 *J. Phys. B: Atom. Molec. Phys.* **2** 26–43
Berrington K A, Bransden B H and Coleman J P 1973 *J. Phys. B: Atom. Molec. Phys.* **6** 436–49
Berrington K A, Burke P G and Sinfailam A L 1975 *J. Phys. B: Atom. Molec. Phys.* **8** 1459–73
Bransden B H and Issa M R 1975 *J. Phys. B: Atom. Molec. Phys.* **8** 1088–94
Chamberlain G E, Mielczarek S R and Kuyatt C E 1970 *Phys. Rev.* A **2** 1905–22
Chan F T and Chen S T 1974 *Phys. Rev.* A **9** 2393–7
Chutjian A 1976 *J. Phys. B: Atom. Molec. Phys.* **9** 1749–56
Chutjian A and Srivastava S K 1975 *J. Phys. B: Atom. Molec. Phys.* **8** 2360–8
Chutjian A and Thomas L D 1975 *Phys. Rev.* A **11** 1583–95
Cohen M and McEachran R P 1969 *J. Phys. B: Atom. Molec. Phys.* **2** 1271–5
Dillon M A and Lassettre E N 1975 *J. Chem. Phys.* **62** 2373–90
Donaldson F G, Hender M A and McConkey J W 1972 *J. Phys. B: Atom. Molec. Phys.* **5** 1192–210
Duxler W M, Poe R T and LaBahn R W 1971 *Phys. Rev.* A **4** 1935–44
Eminyan M, MacAdam K B, Slevin J and Kleinpoppen H 1973 *Phys. Rev. Lett.* **31** 576–9
—— 1974 *J. Phys. B: Atom. Molec. Phys.* **7** 1519–42
Eminyan M, MacAdam K B, Slevin J, Standage M C and Kleinpoppen H 1975 *J. Phys. B: Atom. Molec. Phys.* **8** 2058–66
Flannery M R and McCann K J 1975 *J. Phys. B: Atom. Molec. Phys.* **8** 1716–33
Goldberg L and Clogston A M 1939 *Phys. Rev.* **56** 696–9
Green L C, Mulder M M, Lewis M N and Woll J W Jr 1954 *Phys. Rev.* **93** 787–61
Hall R I, Joyez G, Mazeau J, Reinhardt J and Schermann C 1973 *J. Physique* **34** 827–43
Hidalgo M B and Geltman S 1972 *J. Phys. B: Atom. Molec. Phys.* **5** 617–26
Joachain C J and Vanderpoorten R 1974 *J. Phys. B: Atom. Molec. Phys.* **7** 817–30
de Jongh J P and van Eck J 1971 *Proc. 7th Int. Conf. on Physics of Electronic and Atomic Collisions* (Amsterdam: North Holland) Abstracts pp 701–3
Macek J and Jaecks D H 1971 *Phys. Rev.* A **4** 2288–300
Madison D H and Shelton W N 1973 *Phys. Rev.* A **7** 499–513
McDowell M R C, Morgan L A and Myerscough V P 1973 *J. Phys. B: Atom. Molec. Phys.* **6** 1435–51
——1975a *J. Phys. B: Atom. Molec. Phys.* **8** 1053–72
——1975b *J. Phys. B: Atom. Molec. Phys.* **8** 1838–50
McDowell M R C, Myerscough V P and Narain U 1974 *J. Phys. B: Atom. Molec. Phys.* **7** L195–7
Morse P M, Young L A and Haurwitz E S 1935 *Phys. Rev.* **48** 948–54
Moustafa Moussa H R, de Heer F J and Schutten J 1969 *Physica* **40** 517–49
Opal C B and Beaty E C 1972 *J. Phys. B: Atom. Molec. Phys.* **5** 627–35
Schiff B and Pekeris C L 1964 *Phys. Rev.* **134** A638–40
Scott T 1976 *PhD Thesis* University of London in preparation
Scott T and McDowell M R C 1975a *J. Phys. B: Atom. Molec. Phys.* **8** 1851–65
——1975b *J. Phys. B: Atom. Molec. Phys.* **8** 2369–76
Showalter J G and Kay R B 1975 *Phys. Rev.* A **11** 1899–910
Suzuki H and Takayanagi T 1973 *Proc. 8th Int. Conf. on Physics of Electronic and Atomic Collisions* (Beograd: Institute of Physics) Abstracts pp 286–7
Syms R F, McDowell M R C, Morgan L A and Myerscough V P 1975 *J. Phys. B: Atom. Molec. Phys.* **8** 2817–34
Thomas L D, Csanak G, Taylor H S and Yarlagadda B S 1974 *J. Phys. B: Atom. Molec. Phys.* **7** 1719–33
Truhlar D G, Rice J K, Kupperman A, Trajmar S and Cartwright D C 1970 *Phys. Rev.* A **1** 778–802
Truhlar D G, Trajmar S, Williams W, Ormonde S and Torres B 1973 *Phys. Rev.* A **8** 2475–82
Winters K H 1974 *PhD Thesis* University of Durham
Woollings M J and McDowell M R C 1972 *J. Phys. B: Atom. Molec. Phys.* **5** 1320–31
Yagishita A, Takayanagi T and Suzuki H 1976 *J. Phys. B: Atom. Molec. Phys.* **9** L53–8